



## Convective and absolute instability of a liquid jet in a longitudinal magnetic field

G. A. Shugai and P. A. Yakubenko

Citation: [Physics of Fluids](#) **9**, 1928 (1997); doi: 10.1063/1.869308

View online: <http://dx.doi.org/10.1063/1.869308>

View Table of Contents: <http://scitation.aip.org/content/aip/journal/pof2/9/7?ver=pdfcov>

Published by the [AIP Publishing](#)

---

### Articles you may be interested in

[Absolute/convective instability of planar viscoelastic jets](#)

Phys. Fluids **27**, 014110 (2015); 10.1063/1.4906441

[Absolute-convective instability transition of low permittivity, low conductivity charged viscous liquid jets under axial electric fields](#)

Phys. Fluids **23**, 094108 (2011); 10.1063/1.3637638

[Absolute to convective instability transition in charged liquid jets](#)

Phys. Fluids **22**, 062002 (2010); 10.1063/1.3446972

[Electrohydrodynamic instability of a charged liquid jet in the presence of an axial magnetic field](#)

Phys. Fluids **22**, 044102 (2010); 10.1063/1.3419156

[Transition from convective to absolute instability in a liquid jet](#)

Phys. Fluids **13**, 2732 (2001); 10.1063/1.1387469

---



Launching in 2016!

The future of applied photonics research is here

OPEN  
ACCESS

AIP | APL  
Photonics

# Convective and absolute instability of a liquid jet in a longitudinal magnetic field

G. A. Shugai<sup>a)</sup> and P. A. Yakubenko

Department of Hydraulic Engineering, The Royal Institute of Technology, 100 44 Stockholm, Sweden

(Received 18 September 1996; accepted 17 March 1997)

A circular jet of perfectly conductive inviscid liquid in a uniform longitudinal magnetic field can be absolutely or convectively unstable for different values of the flow parameters. Higher intensity of the field always reduces the domain of absolute instability. For both cases of absolute and convective instability, the corresponding jet of large but finite length is globally unstable if suitable boundary conditions hold at its beginning and end. The unstable global mode is based on a pair of waves that propagate in opposite directions and reflect from one into the other at the flow boundaries. © 1997 American Institute of Physics. [S1070-6631(97)01707-8]

## I. INTRODUCTION

The instability of an infinitely long circular jet of inviscid liquid was analyzed first by Rayleigh.<sup>1</sup> The flow is temporally unstable with respect to any axially symmetric disturbance such that its wavelength is greater than the circumference of the jet.

In practical applications, the jet often flows from a nozzle. Keller *et al.*<sup>2</sup> realized first that the nature of the jet instability problem is rather spatial than temporal. (A summary of the results can be found also in the reviews.<sup>3,4</sup>) Thus, a distinction between absolute and convective type of instability is even more significant than the fact of temporal instability itself—the absolute instability leads to complete disintegration of the flow. In the case of convective instability, the jet can have a sufficiently long continuous part, even though it breaks up into drops farther downstream.

The absolute and convective type of instability for a circular jet of inviscid liquid was investigated analytically by Leib and Goldstein,<sup>5</sup> and experimentally by Monkewitz *et al.*<sup>6</sup> They found that the Weber number used to distinguish absolute from convective instability depends on the shape of the axial velocity profile of the basic flow. A change in the critical value of the Weber number can be also achieved by the inertia of the surrounding medium and the liquid viscosity if they are taken into account.<sup>7,8</sup> The type of instability for a current-carrying jet of low-conductive magnetic liquid was analyzed by Yakubenko.<sup>9</sup>

If the liquid conductivity is high, the flow can be affected by a magnetic field. The temporal instability of a circular jet of perfectly conductive liquid in a uniform longitudinal magnetic field was analyzed by Chandrasekhar.<sup>10</sup> The field reduces the instability and even can completely stabilize the flow.

The jet under consideration often has a finite length in the streamwise direction. One can imagine, for example, a jet that flows from a nozzle and ends at a solid or fluid surface. If the boundary conditions at the flow beginning and end

provide reflection of the disturbances, a self-excited global mode can form. Global instability of a homogeneous jet of large but finite length was analyzed by Yakubenko.<sup>11</sup> The flow can be globally unstable even if the corresponding infinitely long jet is convectively unstable.

The purpose of the present paper is to investigate how a uniform longitudinal magnetic field influences the type of instability for a jet of perfectly conductive inviscid liquid.

## II. FORMULATION

The basic flow is a jet that is straight and circular with a constant radius  $R_0$ . The liquid is inviscid, incompressible with a uniform mass density  $\rho$ , perfectly conductive, and non-magnetic (of magnetic permeability  $\mu_0$ ). The jet velocity  $U_0$  is constant over each cross section. The influences of the gravity and the inertia of the surrounding medium are assumed to be negligible. A uniform magnetic field  $H_0$  is applied parallel to the jet axis (e.g., by a co-axially positioned solenoid). The instability is caused by a surface tension  $\sigma$  that is uniform. The non-dimensional parameters of the system are the Weber number  $We = \sigma / (\rho R_0 U_0^2)$  and  $\alpha = \mu_0 H_0^2 R_0 / (4 \pi \sigma)$ ; the latter is a ratio of the magnetic to capillary forces.

The equations of inviscid magnetohydrodynamics combined with the kinematic and dynamic boundary conditions at the jet surface yield the dispersion relation.<sup>10</sup> For axially symmetric disturbances in the form of monochromatic waves  $A(r) \exp(iKx - i\Omega t)$ , the dispersion relation has two temporal branches that can be represented in the following form:

$$\omega_{\pm} = k \pm [We F(k, \alpha)]^{1/2}, \quad (1)$$

in which

$$F(k, \alpha) = \frac{k}{I_0(k)} \left[ (k^2 - 1) I_1(k) + \frac{\alpha}{K_1(k)} \right], \quad (2)$$

$$k = \text{sign}[\text{Re}(K)] K R_0, \quad (3)$$

$\omega = \Omega R_0 / U_0$ , and  $I_0(k)$ ,  $I_1(k)$  and  $K_1(k)$  are the modified Bessel functions.

Condition (3) implies that the origin in the complex  $k$  plane is a double branch point with two branch cuts along the positive and negative imaginary axes. Therefore, the disper-

<sup>a)</sup>The address for correspondence is G. A. Shugai, Department of Hydraulic Engineering, The Royal Institute of Technology, 100 44 Stockholm, Sweden. Telephone: +46 8 7907956; Fax: +46 8 218116; Electronic mail: galina@versus.ce.kth.se

sion relation is symmetric about the imaginary  $k$  axis, and one needs to consider only the half-plane  $\text{Re}(k) > 0$ .

Only one of the temporal branches, say  $\omega_+(k)$ , exhibits temporally instability, i.e. can have values with positive imaginary parts for real  $k$ . (The subscript for this branch is dropped in the following treatment.)

The flow is temporally unstable<sup>10</sup> if

$$\alpha < 1/2. \quad (4)$$

The region of unstable wavenumbers is a single interval,

$$0 < k < k_{\text{cut}}(We, \alpha). \quad (5)$$

Note that the cutoff wavenumber  $k_{\text{cut}}$  is a branch point of the frequency. If  $\alpha$  increases and  $We$  is kept constant, both  $k_{\text{cut}}$  and the maximum temporal growth rate  $\max_{0 < k < k_{\text{cut}}} \{\text{Im}[\omega(k)]\}$  decrease. Thus, the field reduces temporal instability.

If the disturbance is a wave packet that is initially localized in space, and if some of the waves in the packet grow in time, the entire disturbance can drift downstream and decay in time at every spatial position. The flow is called then convectively unstable; otherwise, it is called absolutely unstable.<sup>12</sup>

The instability type can be determined by investigating on the complex  $k$  plane the so-called saddle points  $k^s$  that are zeros of the group velocity, i.e.,

$$d\omega/dk(k^s) = 0. \quad (6)$$

The saddle points correspond to branch points  $\omega^b$  of the wavenumber on the complex  $\omega$  plane. However, not every saddle point must be taken into account. The additional “pinching requirement” must be satisfied—the corresponding branch point must connect two branches of the wavenumber, which originate from different halves of the complex  $k$  plane.<sup>12</sup> In many cases, the proper saddle points can be found from pure geometric consideration of the structure of the lines  $\text{Im}[\omega(k)] = \text{const}$  on the complex  $k$  plane. In the general case, a special mapping procedure is required.<sup>13</sup> If  $\text{Im}(\omega^b) > 0$  for at least one such point, the instability is absolute.

If the basic flow has a finite length, the boundary conditions typically imply wave reflection at the beginning and end of the flow. Therefore, even “simple” disturbances are superpositions of waves rather than just single waves. If the length of the basic flow  $L$  is large compared to the typical wavelength of the disturbances  $\lambda$ , the global frequencies are approximated up to zeroth order in  $\lambda/L$  by solutions of the following equation:<sup>12,14,15</sup>

$$\min_m \{\text{Im}[k_m(\omega)]\} = \max_n \{\text{Im}k_n(\omega)\}, \quad (7)$$

in which the minimum and maximum are taken, respectively, among the waves that propagate downstream and upstream. Additionally, the boundary conditions must guarantee that two corresponding waves can reflect from one into the other.

Note that Eq. (7) is a real relation for a complex quantity  $\omega$ . Therefore, it defines a continuous curve  $C$  in the complex  $\omega$  plane. However, the first-order correction term appears to

be discrete.<sup>14</sup> The global frequencies are located in the complex  $\omega$  plane at distances  $O(\lambda/L)$  from the curve  $C$ . Thus, the condition

$$\max_C [\text{Im}(\omega)] \gg \lambda/L, \quad (8)$$

is sufficient for global instability.

### III. RESULTS

#### A. Spatial branches

The spatial stability analysis requires frequency to be real; the wavenumber branches  $k(\omega)$  represent then spatial amplifying or decaying waves.

In contrast to the frequency, the wavenumber cannot be explicitly expressed from the dispersion relation (1). However, for  $We \ll 1$ , the spatial branches can be calculated approximately. If the following series expansion is applied:

$$k = \sum_{m=0}^{\infty} We^{m/2} k^{(m)}, \quad (9)$$

the dispersion relation (1) gives in the lowest order in  $We$ ,

$$(\omega - k^{(0)})^2 I_0(k^{(0)}) K_1(k^{(0)}) = 0. \quad (10)$$

Since  $K_1(k)$  has no roots such that  $\text{Re}(k) \geq 0$ , all roots of (10) are given by

$$k^{(0)} = \omega, \quad (11)$$

$$\hat{k}^{(0)} = \pm i j_{0,n}, \quad n = 1, 2, \dots, \quad (12)$$

in which  $j_{0,n}$  is the  $n$ th positive root of the Bessel function  $J_0$ . Other coefficients in the series (9) can be then computed recursively. For the root (11), one has two branches:

$$k_{1,2}(\omega) = \omega \mp We^{1/2} F^{1/2}(\omega, \alpha) + We G(\omega, \alpha) + O(We^{3/2}), \quad (13)$$

in which minus and plus signs are taken for  $k_1(\omega)$  and  $k_2(\omega)$ , respectively,  $F(\omega, \alpha)$  is the same as in Eq. (1), and

$$G(\omega, \alpha) = \omega^2 \frac{I_1(\omega)}{I_0(\omega)} - \frac{1}{2} \omega(\omega^2 - 1) \left[ \frac{I_1^2(\omega)}{I_0^2(\omega)} - 1 \right] + \frac{\alpha}{2I_0(\omega)K_1(\omega)} \left[ \frac{I_1(\omega)}{I_0(\omega)} - \frac{K_0(\omega)}{K_1(\omega)} - 2 \right]. \quad (14)$$

In addition, for the roots (12), one has the following branches:

$$\begin{aligned} \hat{k}_{\pm n}(\omega) = & \pm i j_{0,n} + We \frac{j_{0,n}}{(\omega^2 + j_{0,n}^2)^2} [2\omega j_{0,n} \mp i(\omega^2 - j_{0,n}^2)] \\ & \times \left\{ j_{0,n}^2 + 1 + \frac{\alpha}{I_1(\pm i j_{0,n})K_1(\pm i j_{0,n})} \right\} + O(We^2), \end{aligned} \quad (15)$$

in which  $n = 1, 2, \dots$ . If  $\alpha = 0$ , Eqs. (13) and (15) yield Eqs. (12) and (13) of Keller *et al.*<sup>2</sup>

However,  $We \ll 1$  introduces a singular perturbation into the dispersion relation. Thus, in addition to (9), the following singular expansion is applied:

$$k = \sum_{m=-2}^{\infty} We^{m/2} k^{(m)}. \quad (16)$$

Then, two more branches are obtained,

$$k_{-1,-2}(\omega) = \pm We^{-1} \pm \left( \frac{1}{2} - 2\alpha \right) - 2\omega + We \left[ \pm \left( \frac{9}{8} - 3\omega^2 - \frac{\alpha}{2} \right) + \omega(1-4\alpha) \right] + O(We^2), \quad (17)$$

in which plus and minus signs are taken for  $k_{-1}(\omega)$  and  $k_{-2}(\omega)$ , respectively.

Strictly speaking, asymptotic formulas (13)–(17) are not valid for large  $|\omega|$ . However, our numerical investigations of the dispersion relation show that the indexation of spatial branches, which is used in (13)–(17), remain reasonable for finite values of  $\text{Im}(\omega) > 0$  and finite values of  $We$ . Thus, the following conclusions hold.

For  $\text{Im}(\omega) > 0$ , one has  $\text{Im}[k_{1,2}(\omega)] > 0$ ,  $\text{Im}[k_{-1,-2}(\omega)] < 0$ ,  $\text{Im}[\hat{k}_n(\omega)] > 0$ , and  $\text{Im}[\hat{k}_{-n}(\omega)] < 0$  for any  $n > 0$ ; see Fig. 1. Therefore, the branches with positive and negative indexes correspond to the waves that propagate downstream and upstream, respectively. Note that  $\text{Re}[k_{-2}(\omega)] < 0$  for  $\text{Im}(\omega) \geq 0$ , so that the branch  $k_{-2}(\omega)$  must not be considered because of the condition (3).

Furthermore, for  $\text{Im}(\omega) \geq 0$ , any branches except  $k_1(\omega)$  never cross the real  $k$  axis, so that the corresponding waves are always spatially damped in their direction of propagation. For  $k_1(\omega)$ , one has  $\text{Im}[k_1(\omega)] < 0$  at real  $\omega$  such that  $0 < \omega < \omega_{\text{cut}}(We, \alpha)$ ; see Fig. 2. The corresponding wave is then spatially amplified in its direction of propagation. If  $k$  and  $\omega$  are swapped, dispersion relation (1) becomes identical to Eq. (13) up to the order of  $We^{1/2}$ . Therefore,  $\omega_{\text{cut}}(We, \alpha) \approx k_{\text{cut}}(We, \alpha)$  for  $We \ll 1$ .

## B. Absolute vs convective instability

Equations (1) and (6) give the following equation for the saddle points:

$$We = 4F(k^s, \alpha) \left/ \left[ \frac{\partial F}{\partial k}(k^s, \alpha) \right]^2 \right. \quad (18)$$

Two saddle points are found to determine the structure of the lines  $\text{Im}[\omega(k)] = \text{const}$  near the real  $k$  axis. The saddle points correspond to the branch points of three spatial branches  $k_1(\omega)$ ,  $k_2(\omega)$ , and  $k_{-1}(\omega)$ .

In the case of absolute instability [Fig. 1(a)], two saddle points  $k_{-1,1}^s$  and  $k_{-1,2}^s$  are complex conjugates in the complex  $k$  plane, and

$$\text{Im}(\omega_{-1,1}^b) = -\text{Im}(\omega_{-1,2}^b) > 0. \quad (19)$$

(Here and below, the double indexes for the saddle points  $k_{p,q}^s$  and the corresponding branch points  $\omega_{p,q}^b$  are given in connection with the corresponding spatial branches.)

In the case of convective instability [Fig. 1(b)], the saddle points  $k_{1,2}^s$  and  $k_{-1,2}^s$  are located at the real axis, and

$$\text{Im}(\omega_{1,2}^b) = \text{Im}(\omega_{-1,2}^b) = 0. \quad (20)$$

Note that  $\omega_{1,2}^b = \omega_{\text{cut}}(We, \alpha)$ .

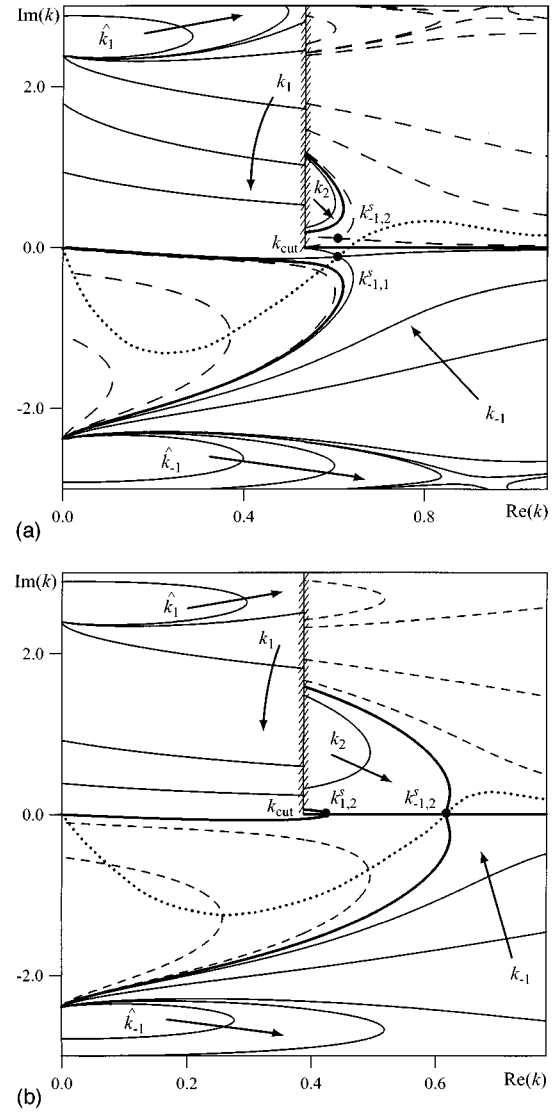


FIG. 1. Contour plots  $\text{Im}[\omega(k)] = \text{const}$  for  $We = 1$  and (a)  $\alpha = 0.3$  (absolute instability), (b)  $\alpha = 0.38$  (convective instability). The solid, dashed, and bold lines are for positive, negative, and zero values of  $\text{Im}[\omega(k)]$ , respectively. The steepest descent contours are shown by the dotted lines. The slashed lines are for the branch cuts. The arrows present movements of the spatial branches as  $\text{Im}(\omega)$  decreases.

At the onset of the absolute instability, the saddle points coincide at the real  $k$  axis and form a double saddle point, so that

$$d^2\omega/dk^2(k^s) = 0. \quad (21)$$

Equations (1) and (21) yield

$$2F(k^s, \alpha) \frac{\partial^2 F}{\partial k^2}(k^s, \alpha) = \left[ \frac{\partial F}{\partial k}(k^s, \alpha) \right]^2, \quad (22)$$

which is independent of  $We$ . Using Eq. (18), the absolute instability criterion can be expressed in the following form:

$$We > We_{\text{abs}}(\alpha) = 2 \left/ \frac{\partial^2 F}{\partial k^2}(k^s, \alpha) \right., \quad (23)$$

in which  $k^s$  can be found numerically for every  $\alpha$  from Eq. (22). The domains of absolute and convective instability on

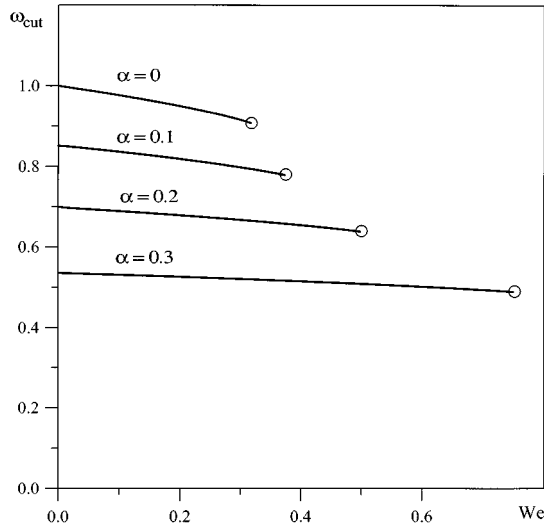


FIG. 2. The real frequency cutoff for spatial instability. The circled end of each curve corresponds to  $We = We_{abs}(\alpha)$ , see Fig. 3.

the  $(\alpha, We)$  plane are shown in Fig. 3. Higher intensity of the field always reduces the domain of absolute instability, while higher surface tension always enlarges it. For  $\alpha = 0$ , one has  $We_{abs} \approx 0.32$ , which is the result of Leib and Goldstein.<sup>5</sup>

### C. Global instability

The boundary conditions at the beginning and end of the jet are assumed to allow to find the amplitude of every outgoing wave if the amplitudes of the incoming waves are specified. This very broad assumption appears to be sufficient for the global instability analysis;<sup>14</sup> a discussion of its

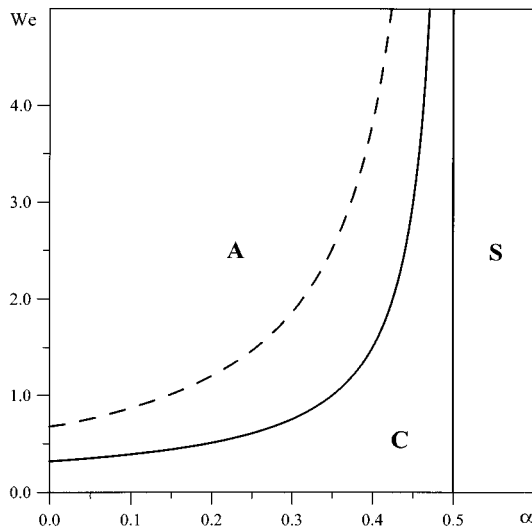


FIG. 3. The domains bounded by the solid lines and marked by (S), (A), and (C) correspond to stability, absolute, and convective instability, respectively. The maximum growth rate of the global mode is greater than the increment of absolute instability if  $We < We_*(\alpha)$ , which is shown by the dashed line.

physical workability is given in Section IV; possible particular forms of the boundary conditions can be found in the review.<sup>4</sup>

The global frequency selection criterion (7) leads to the equation

$$\text{Im}[k_1(\omega) - k_{-1}(\omega)] = 0, \quad (24)$$

which defines a curve  $C$  in the complex  $\omega$  plane. If this curve has points in the upper half-plane, the flow is globally unstable. The maximal growth rate of the global mode is then

$$\omega_i^G \equiv \max_C [\text{Im}(\omega)]. \quad (25)$$

In the case of absolute instability, i.e., for  $We > We_{abs}(\alpha)$ , two different situations occur. If  $We > We_*(\alpha)$ , then  $\omega_i^G = \text{Im}(\omega_{-1,1}^b)$ , the latter is a growth rate of disturbances for the case of absolute instability for an infinitely long jet. (One often calls  $\omega_{-1,1}^b$  the absolute frequency.)

For  $We < We_*(\alpha)$ , one has  $\omega_i^G > \text{Im}(\omega_{-1,1}^b)$ . Hence, the growth rate of the global mode is greater than the increment of absolute instability. The plot of  $We_*(\alpha)$  is shown in Fig. 3. For  $\alpha = 0$ , one has  $We_*(0) \approx 0.68$ , which is the result of Yakubenko.<sup>11</sup>

In the case of absolute instability, i.e., for  $We < We_{abs}(\alpha)$ , the branch points  $\omega_{1,2}^b$  and  $\omega_{-1,2}^b$  are located at the real  $\omega$  axis. For  $\omega = 0$  and for real  $\omega$  such that  $\omega_{1,2}^b < \omega < \omega_{-1,2}^b$ , one has  $\text{Im}[k_1(\omega)] = \text{Im}[k_{-1}(\omega)] = 0$ . If real  $k$  increases from  $k_{cut}$  to  $k_{1,2}^s$ , then  $d\omega(k)/dk$  monotonically increases from  $-\infty$  to 0. If  $k$  increases from  $k_{-1,2}^s$  to  $+\infty$ , then  $d\omega(k)/dk$  monotonically decreases from 0 to  $-\infty$ . Therefore, real  $\omega^*$  exists such that  $\omega_{-1,2} < \omega^* < \omega_{1,2}$  and

$$\frac{d\omega}{dk}[k_1(\omega^*)] = \frac{d\omega}{dk}[k_{-1}(\omega^*)]. \quad (26)$$

If  $k_1(\omega)$  and  $k_{-1}(\omega)$  are expanded into a Taylor series in the neighborhood of  $\omega^*$ ,

$$\begin{aligned} \text{Im}[k_1(\omega) - k_{-1}(\omega)] \approx & \frac{1}{2} \left\{ \frac{d^2\omega}{dk^2}[k_1(\omega^*)] \right. \\ & \left. - \frac{d^2\omega}{dk^2}[k_{-1}(\omega^*)] \right\} \text{Im}[(\omega - \omega^*)^2]. \end{aligned} \quad (27)$$

Therefore, Eq. (24) is satisfied in the complex  $\omega$  plane at two locally perpendicular lines that cross each other at  $\omega^*$ . Since one of the lines is a segment of the real  $\omega$  axis, the other one must have points in the half-plane  $\text{Im}(\omega) > 0$  (see Fig. 4). Hence, the flow is globally unstable, even though the corresponding infinitely long jet is convectively unstable for  $We < We_{abs}(\alpha)$ .

For  $We \ll 1$ , Eqs. (13) and (17) give the following equation for the global frequencies:

$$\begin{aligned} 3\text{Im}(\omega) - We^{1/2}\text{Im}[F^{1/2}(\omega, \alpha)] + We\text{Im}[G(\omega, \alpha) + 3\omega^2 \\ - \omega(1 - 4\alpha)] = O(We^{3/2}). \end{aligned} \quad (28)$$

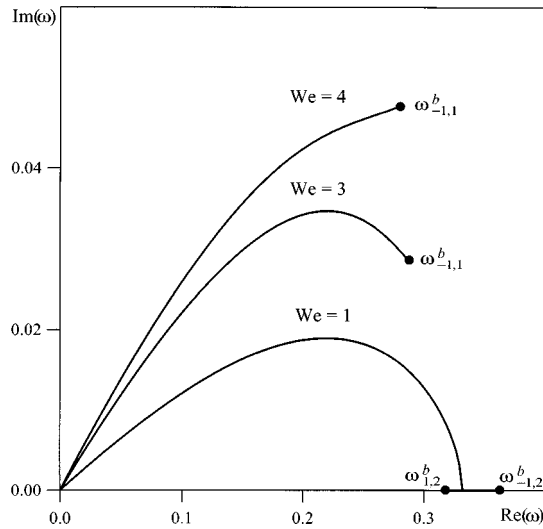


FIG. 4. Solutions for  $\alpha=0.4$  of Eq. (24) that approximates the spectrum of global frequencies.

Although the global mode is based on the branches  $k_1(\omega)$  and  $k_{-1}(\omega)$ , the corresponding waves form only a “skeleton” of it. The mode itself involves also all other waves if they can be excited at the boundaries.

#### IV. CONCLUSIONS AND DISCUSSION

A circular jet of inviscid, incompressible, and perfectly conductive liquid in a uniform longitudinal magnetic field can be temporally unstable. The instability can be then absolute or convective for different values of the flow parameters. Higher intensity of the field always reduces the domain of absolute instability, while higher surface tension always enlarges it.

In the case of moderately large conductivity, we expect the restoring effect of the magnetic field to be weaker, since the force lines are then only partially frozen into the medium. More sophisticated analysis of the dispersion relation is required for this case, since even the temporal branches cannot any more be explicitly obtained.<sup>10</sup>

In both cases of absolute and convective instability, our analysis shows that the corresponding jet of large but finite length is globally unstable. The magnetic field only reduces

the growth rate of the global mode. A natural physical question arises, why this instability does not appear often when, e.g., a jet from a tube hits a wash-basin?

A global mode forms only if the waves  $k_1$  and  $k_{-1}$  that correspond to the spatial branches  $k_1(\omega)$  and  $k_{-1}(\omega)$  can be properly reflected from one into the other at the flow beginning and end. For  $We \ll 1$ , the branches are  $k_1(\omega) \approx \omega$  and  $k_{-1}(\omega) \approx 1/We$  according to Eqs. (13) and (17). Therefore, the wavelength of  $k_{-1}$  is much shorter than the wavelength of  $k_1$ , and the required reflection scheme can be upset. In addition, the effect of viscosity might become important for the dynamics of the wave  $k_{-1}$ . On the other hand, for  $We$  close to the onset of absolute instability  $We_{abs}$ , the wavelengths of both  $k_1$  and  $k_{-1}$  are of order of the jet diameter, so that the global mode should form. However, the onset of possible non-linear growth of the mode can be somewhat obscured by the transition to absolute instability.

<sup>1</sup>Lord Rayleigh, “On the instability of jets,” *Proc. London Math. Soc.* **10**, 4 (1878).

<sup>2</sup>J. B. Keller, S. I. Rubinow, and Y. O. Tu, “Spatial instability of a jet,” *Phys. Fluids* **16**, 2052 (1973).

<sup>3</sup>N. Ashgriz and F. Mashayek, “Temporal analysis of capillary jet breakup,” *J. Fluid Mech.* **291**, 163 (1995).

<sup>4</sup>D. B. Bogoy, “Drop formation in a circular liquid jet,” *Annu. Rev. Fluid Mech.* **11**, 207 (1979).

<sup>5</sup>S. J. Leib and M. E. Goldstein, “The generation of capillary instability on a liquid jet,” *J. Fluid Mech.* **168**, 479 (1986).

<sup>6</sup>P. A. Monkewitz *et al.*, “The breakup of a liquid jet at high Weber number,” *Bull. Am. Phys. Soc.* **33**, 2273 (1988).

<sup>7</sup>S. J. Leib and M. E. Goldstein, “Convective and absolute instability of a viscous liquid jet,” *Phys. Fluids* **29**, 952 (1986).

<sup>8</sup>S. P. Lin and Z. W. Lian, “Absolute instability of a liquid jet in a gas,” *Phys. Fluids A* **1**, 490 (1989).

<sup>9</sup>P. A. Yakubenko, “Absolute and convective instability of current-carrying jet of magnetic liquid,” *Eur. J. Mech. B Fluids* **14**, 823 (1995).

<sup>10</sup>S. Chandrasekhar, *Hydrodynamic and Hydromagnetic Stability* (Clarendon Press, Oxford, 1961).

<sup>11</sup>P. A. Yakubenko, “Capillary instability of an ideal jet of large but finite length,” *Eur. J. Mech. B Fluids* **16**, 39 (1997).

<sup>12</sup>A. Bers, “Space-time evolution of plasma instabilities—absolute and convective,” in *Handbook of Plasma Physics*, edited by M. N. Rosenbluth and R. Z. Sagdeev (North-Holland, Amsterdam, 1983), Vol. I, pp. 501–515.

<sup>13</sup>K. Kupfer, A. Bers, and A. K. Ram, “The cusp map in the complex-frequency plane for absolute instability,” *Phys. Fluids* **30**, 3075 (1987).

<sup>14</sup>A. G. Kulikovskii, “On the stability of homogeneous states,” *J. Appl. Math. Mech.* **30**, 180 (1966).

<sup>15</sup>E. M. Lifshitz and L. P. Pitaevskii, *Physical Kinetics* (Pergamon Press, Oxford, 1981), pp. 281–283.